Surface Science Letters

Wulff shape of strontium titanate nanocuboids

CrossMark

Lawrence Crosby [a,*], James Enterkin [b], Federico Rabuffetti [c], Kenneth Poeppelmeier [b], Laurence Marks [a]

[a] Department of Materials Science and Engineering, Northwestern University, Evanston, IL 60208, United States
[b] Department of Chemistry, Northwestern University, Evanston, IL 60208, United States
[c] Department of Chemistry, Wayne State University, Detroit, MI 48202, United States

ARTICLE INFO

ABSTRACT

Here we describe the Wulff shape of strontium titanate nanocuboids prepared by a hydrothermal method and annealed at high temperature. Transmission electron microscopy was used to measure the faceting ratios $d_{(110)}:d_{(100)}$ which are compared with surface energy ratios $\gamma_{(110)}:\gamma_{(100)}$ from first-principles calculations. Internal voids attributed to the Kirkendall effect were also measured and show agreement with the external faceting. Experiment and theory are shown to agree strongly within statistical and density functional theory error.

© 2014 Elsevier B.V. All rights reserved.

1. Introduction

Oxide materials have been developed for a broad array of applications ranging from catalysis [1], to dielectrics [2], ferroelectrics [3], and transparent conductors [4,5]. One material which has been studied in detail is strontium titanate (SrTiO$_3$ or STO) due to its prototypical cubic perovskite crystal structure [6] and its widespread use as a substrate for growth of thin films. There have been several works published regarding synthesis of STO in various nanoscale morphologies [7–9]. In spite of the considerable volume of literature on the subject, there is limited understanding of the properties of STO in nanoparticle form. It is also important to consider that surfaces are distinct from the bulk due to the loss of coordination going from an "infinite" periodic structure to an abrupt termination of the said periodicity [10]. Given that the surface-to-volume ratio increases as particle size decreases, the properties of STO nanoparticles could be quite different from bulk STO.

It is well-known that the nanoparticle shape is thermodynamically controlled by the thermodynamic Wulff construction [11]. This is the surface that minimizes the total surface free energy of a crystal, and is found by taking the inner envelope of tangents of the surface energy as a function of crystallographic orientation. As such, the coverage of different facets will be fixed for a particular material system in thermodynamic equilibrium [12].

In this note we report the Wulff shape of STO annealed in air using electron microscopy to measure both the external shape as well as that of the internal Kirkendall voids (Fig. 1).

2. Methods

Strontium titanate nanocuboids were prepared by hydrothermal synthesis as described elsewhere [13–16]. The samples were dispersed on SiN TEM grids and subsequently annealed at different temperatures (700 °C to 950 °C in steps of 50 °C) for various times
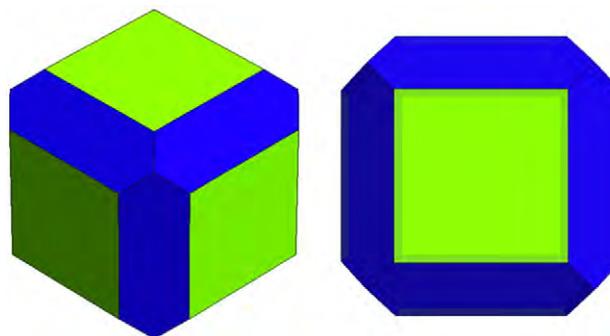
Fig. 1. Observed octadecahedral shape of SrTiO$_3$ nanoparticles. Note that the coverage of the six {100} facets (green) dominates and thus they are described as nanocuboids. The shape was calculated using the WulffMaker Mathematica code [29] for the $d_{(110)}:d_{(100)}$ ratio of 1.139.

* Corresponding author.
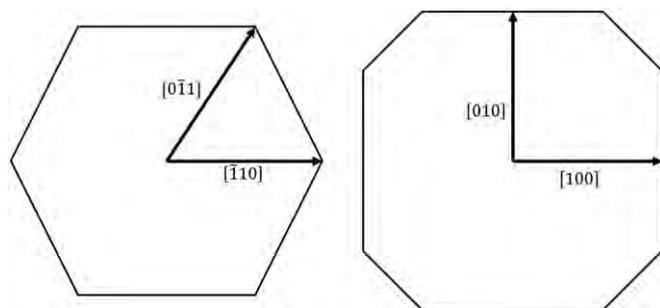E-mail address: crosbyla@u.northwestern.edu (L. Crosby).

Fig. 2. Projection of nanocuboid along left [111] zone axis and right [001] zone axis.

Table 1
Measured $d_{(110)}$:$d_{(100)}$ ratios for nanocuboids following various annealing conditions.

Annealing conditions	# Cuboids measured	Mean $d_{(110)}$:$d_{(100)}$ ratio	Standard deviation	Margin of error
700 °C, 5 h, Air	2	1.173	0.032	0.286
750 °C, 10 h, Air	3	1.130	0.039	0.096
800 °C, 5 h, Air	3	1.198	0.038	0.342
950 °C, 2 h, O_2	8	1.140	0.026	0.052
950 °C, 5 h, O_2	6	1.160	0.050	0.022
950 °C, 20 h, O_2	9	1.107	0.086	0.066
Total	29	1.139	0.055	0.045

in a fused silica tube within a tube furnace. A JEOL JEM-2100 FasTEM was used for TEM imaging and electron diffraction (TED) measurements. The TED measurements were used to determine the crystallographic orientation and characterize defects in the nanocuboids. Diffraction patterns were captured using the CCD camera on the microscope and averaged over several exposures.

Calculations for the observed Wulff shape were carried out by measuring the distance from the center of several nanocuboids to the respective face (either (100) or (110) in our case) and yielded the $d_{(110)}$:$d_{(100)}$ ratios which are proportional to the ratios of surface free energy per area (Fig. 2). All nanocuboids analyzed in this fashion were imaged near to the [001] zone axis and the arithmetic mean of several measurements was calculated for each anneal temperature (see Table 1).

DFT calculations were performed with the all-electron augmented plane wave + local orbitals WIEN2K code [17]. The surface in-plane lattice parameters were set to those of the corresponding DFT optimized bulk cell, with ~1.6 nm of vacuum to avoid errors within the DFT calculations as well as in the STM simulations, the latter being done using the Tersoff–Hamann approximation [18]. Muffin-tin radii were set to 1.55, 2.36 and 1.75 bohr for O, Sr and Ti respectively, as well as a min(RMT) $* K_{max}$ of 7.0, with a $3 \times 3 \times 1$ Brillouin-zone reciprocal space sampling of the primitive unit cell. The electron density and atomic positions were simultaneously converged using a quasi-Newton algorithm [19]; the numerical convergence was better than 0.01 eV/1×1 surface cell. The PBEsol [20] generalized gradient approximation as well as the revTPSS method [21] was used, with 0.5 on-site exact-exchange the optimized number for several test TiO_x molecules similar to earlier work [22]. The surface enthalpy per (1×1) surface unit cell (E_{surf}) was calculated as: $E_{surf} = (E_{slab} - E_{STO} * N_{STO} - E_{TO} * N_{TO})$ / ($2 * N_{1x1}$), where E_{slab} is the total enthalpy of the slab, E_{STO} for one bulk $SrTiO_3$ unit cell, N_{STO} the number of bulk $SrTiO_3$ unit cells, E_{TO} bulk rutile TiO_2, N_{TO} the number of excess TiO_2 units and ($N_{1 \times 1}$) the number of (1×1) cells. Consistency checks between the different functionals indicated an error in the energies of approximately 0.1 eV/1×1 cell (~60 mJ/m^2, 8 kJ/mol).

As a caveat, DFT calculations are substantially better for relative energies than absolute ones. Common, simple functionals badly overestimate the covalency, leading to too much hybridization of the oxygen 2p and metal d states. While it is common to use LDA + U methods to correct this, we prefer an on-site exact exchange method as this leads to an effective U which varies as a function of metal co-ordination and so is more appropriate. In addition to this, the use of a metaGGA leads to a much better treatment of the states at surfaces, and much better surface errors. However, there will still be systematic errors, for instance the non-bonded O–O repulsions which are probably under-estimated.

3. Results

The results of TEM imaging reveal a general cubic morphology with the (100) facets dominating, but with additional significant coverage of (110) faces. The nanocuboids were single crystals as evidenced by the nanodiffraction measurements (see Fig. 3). HREM demonstrates that faces which appear flat at low magnifications have many defects and step edges, which are a combination of the (100) and (110) faces. There were also defects present within the nanocuboids with the same shape and faceting as the exterior surfaces. Thickness mapping measurements showed that these areas were thinner than the rest of the nanocuboids and thus they were identified as voids or cavities. Such voids have been observed in other work ([23,24]), and in our
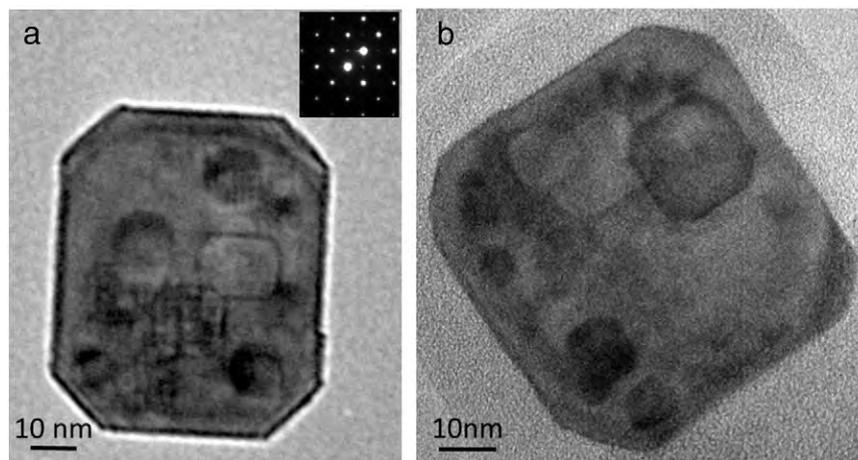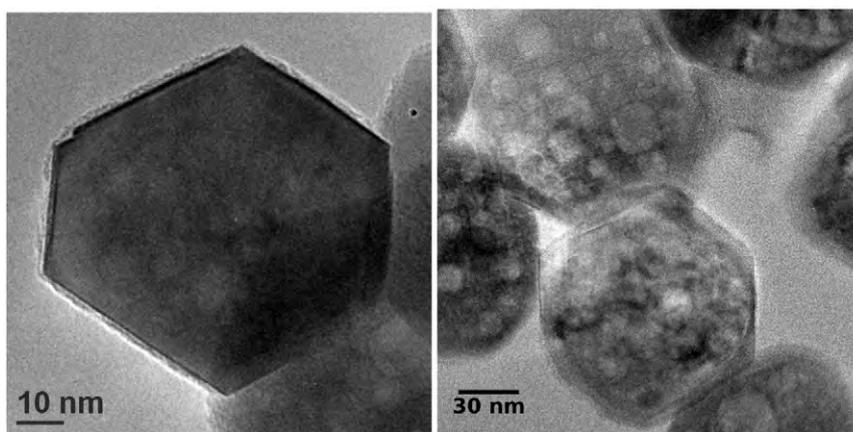

Fig. 3. TEM images of annealed nanocuboids along [001] zone axis demonstrating distinct (100) and (110) faceting that is characteristic of the Wulff shape, in a) annealed at 700 °C and b) 900 °C.

Fig. 4. TEM Images of several nanocuboids (also annealed) near [111] zone axis. Note that in both images, the projected shape is hexagonal, indicating that no substantial (111) faceting is present.
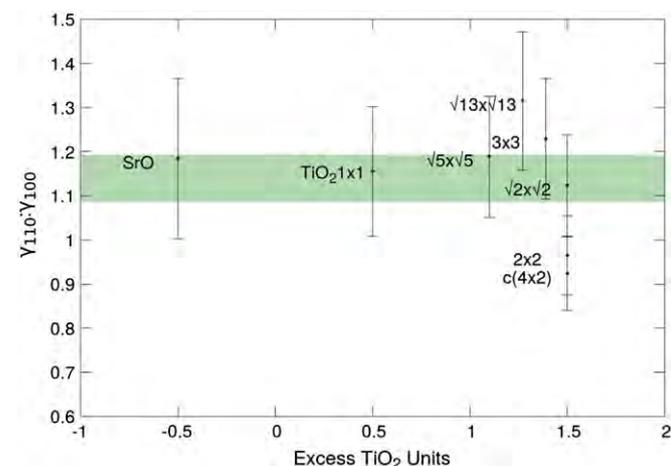
case it is likely that they result from interdiffusion of the strontium precursor into an amorphous titanium complex [25] during the hydrothermal treatment.

A table with measurements of $d_{(110)}$:$d_{(100)}$ ratios for various annealing temperatures appears below (Table 1). The average $d_{(110)}$:$d_{(100)}$ ratio calculated is 1.139 with a standard deviation of 0.055. With a high degree of statistical confidence, increasing the annealing temperature had no effect on the faceting. However, it did reduce the corner rounding and faceting by reducing the number of surface steps. Samples annealed at 700 °C exhibited distinct (110) faceting at the corners (see Fig. 3a). Increasing the temperature further resulted in smoother (100) and (110) faces (e.g. Fig. 3b) until the point that surface roughening occurred at 1100 °C. The voids observed in the as-prepared samples remained after the annealing process. The voids measured were found to exhibit the same faceting as the external surfaces, and the size remained the same after annealing (see Fig. 3).

A careful analysis of a number of particles using images near the [111] and [110] zone axes indicated that there was no evidence of any (111) facets, and very little of any other type of exposed surface excepting some rounding of what would otherwise be sharp corners (see Figs. 3 and 4).

4. Discussion

The fact that the nanocuboids largely maintained their shape before and after annealing as evidenced by the $d_{(110)}$:$d_{(100)}$ ratios remaining statistically unchanged indicates that the shape we have observed is

the thermodynamic limit and is representative of the Wulff construction. Other shapes have been observed such as the cubic morphology in which the (100) surfaces dominate, but the synthesis surfactant is likely a limiting reagent for crystallization on the (110) surfaces, and as such a predominantly kinetic effect. In our case, the annealing process provides an explanation for the stabilization of the (110) facets both on the surfaces of the nanocuboids and internally in the voids.

The comparison of the experimental results with DFT calculations is very informative, remembering that the latter are better at yielding relative energies than absolute values. A table of calculated surface energy ratios for various surface structures on (100) and (110) surfaces based upon the DFT calculations is given in Fig. 5. A more complete comparison to experiment is to compare the ratio $\gamma_{(110)}$:$\gamma_{(100)}$, using an error of 0.13 for the DFT calculations based upon an uncertainty of 0.1 eV/1 × 1 unit cell. Based upon recent work [26] the samples should be near the composition of the √13 × √13 reconstruction [27], perhaps co-existing with some SrO 1 × 1 termination. For the (110) surface energy we used a linear combination of the 1 × 1 oxygen terminated surface and the 3 × 1 surface [28].

The agreement is reasonable, although the ratio expected from the DFT calculations is larger than one would expect for a √13 × √13 reconstruction.

Fig. 5. $\gamma_{(110)}$:$\gamma_{(100)}$ ratios from first-principles calculations compared within one standard deviation of the mean observed $d_{(110)}$:$d_{(100)}$ ratio of 1.139.

References

[1] A.R.J.H. Voorhoeve, D.W. Johnson, J.P. Remeika, P.K. Gallagher, Science 195 (1977) 827.
[2] G. Arlt, D. Hennings, G.d. With, J. Appl. Phys. 58 (4) (1985) 1619–1625.
[3] K. Kiss, J. Magder, M.S. Vukasovich, R.J. Lockhart, J. Am. Ceram. Soc. 49 (1966) 291.
[4] L. Goris, R. Noriega, M. Donovan, J. Jokisaari, G. Kusinski, a Salleo, J. Electron. Mater. 38 (2009) 586.
[5] A. Klein, C. Körber, A. Wachau, F. Säuberlich, Y. Gassenbauer, S.P. Harvey, D.E. Proffit, T.O. Mason, Transparent conducting oxides for photovoltaics: manipulation of fermi level, work function and energy band alignment, materials, 3 (2010) 4892.
[6] A. Bhalla, R. Guo, R. Roy, Mater. Res. Innov. (2000) 3.
[7] K. Fujinami, K. Katagiri, J. Kamiya, T. Hamanaka, K. Koumoto, Nanoscale 2 (2010) 2080.
[8] U.a. Joshi, J.S. Lee, Small (Weinheim an der Bergstrasse, Germany) 1 (2005) 1172.
[9] J. Urban, W. Yun, Q. Gu, H. Park, J. Am. Chem. Soc. 124 (2002) 1186.
[10] G.A. Somorjai, Principles of Surface Chemistry, 1972.
[11] G. Wulff, Zeitschrift fur Krystallographie und Mineralogie 34 (1901) 449.

[12] S. Miracle-Sole, Wulff shape of equilibrium crystals, arXiv, preprint arXiv:1307. 51802013. 1.

[13] F.A. Rabuffetti, H.S. Kim, J.A. Enterkin, Y.M. Wang, C.H. Lanier, L.D. Marks, K.R. Poeppelmeier, P.C. Stair, Chem. Mater. 20 (2008) 5628.

[14] S.T. Christensen, J.W. Elam, F.A. Rabuffetti, Q. Ma, S.J. Weigand, B. Lee, S. Seifert, P.C. Stair, K.R. Poeppelmeier, M.C. Hersam, M.J. Bedzyk, Small 5 (2009) 750.

[15] J.A. Enterkin, K.R. Poeppelmeier, L.D. Marks, Nanoletters 11 (2011) 993.

[16] F.A. Rabuffetti, P.C. Stair, K.R. Poeppelmeier, J. Phys. Chem. C 114 (2010) 11056.

[17] P. Blaha, K. Schwarz, G. Madsen, D. Kvasnicka, J. Luitz, Wien2k, An Augmented Plane Wave + Local Orbitals Program for Calculating Crystal Properties, Techn. Universität Wien, Austria, 2001.

[18] J. Tersoff, D.R. Hamann, Phys. Rev. Lett. 50 (1983) 1998.

[19] L.D. Marks, J. Chem. Theory Comput. 9 (2013) 2786.

[20] J.P. Perdew, A. Ruzsinszky, G.I. Csonka, O.A. Vydrov, G.E. Scuseria, L.A. Constantin, X.L. Zhou, K. Burke, Phys. Rev. Lett. 100 (2008).

[21] V.N. Staroverov, G.E. Scuseria, J. Tao, J.P. Perdew, J. Chem. Phys. 119 (2003) 12129.

[22] D.M. Kienzle, A.E. Becerra-Toledo, L.D. Marks, Phys. Rev. Lett. 106 (2011).

[23] A.D. Smigelskas, E.O. Kirkendall, AIME Trans. 171 (1947) 130.

[24] J. Chen, K. Huang, S. Liu, Electrochim. Acta 55 (2009) 1.

[25] Y. Zhu, L. Zhang, C. Gao, L. Cao, J. Mater. Sci. 5 (2000) 4049.

[26] Y. Lin, J. Wen, L. Hu, R.M. Kennedy, P.C. Stair, K.R. Poeppelmeier, L.D. Marks, Phys. Rev. Lett. 111 (2013) 156101.

[27] D.M. Kienzle, A.E. Becerra-Toledo, L.D. Marks, Phys. Rev. Lett. 106 (2011) 176102.

[28] J.A. Enterkin, A.K. Subramanian, B.C. Russell, M.R. Castell, K.R. Poeppelmeier, L.D. Marks, Nat. Mater. 9 (2010) 245.

[29] R.V. Zucker, D. Chatain, U. Dahmen, S. Hagège, W.C. Carter, J. Mater. Sci. 47 (2012) 8290.